High-resolution L-shell Auger spectroscopy of Mg-like scandium produced in 89-MeV Sc^{8+} + He collisions

M. Sataka, K. Kawatsura,* H. Naramoto, and Y. Nakai
Department of Physics, Japan Atomic Energy Research Institute, Tokai, Ibaraki 319-11, Japan

Y. Yamazaki, K. Komaki, and K. Kuroki
Institute of Physics, College of Arts and Sciences, University of Tokyo, Tokyo 153, Japan

Y. Kanai, T. Kambara, and Y. Awaya
The Institute of Physical and Chemical Research (RIKEN), Wako, Saitama 351-01, Japan

J. E. Hansen
Zeeman Laboratorium, Universiteit van Amsterdam, Plantage Muidergracht 4, NL-1018 TV Amsterdam, The Netherlands

I. Kádár† and N. Stolterfoht
Hahn-Meitner Institut, Bereich Kern und Strahlenphysik, D-1000 Berlin 39, Federal Republic of Germany
(Received 27 June 1991)

In 89-MeV Sc^{8+} + He collisions, the light target atom He was used to ionize selectively the $2p$ shell of the scandium projectile. The subsequent L-shell Auger emission from Mg-like Sc^{9+} was measured with high resolution using the method of zero-degree Auger spectroscopy. The spectra are dominated by three peak groups that are attributed to transitions from the various initial states belonging to the configuration $1s^2 2s^2 2p^5 3s^2 3p$ to the final states $1s^2 2s^2 2p^6 3s\ ^2S$, $1s^2 2s^2 2p^6 3p\ ^2P$, and $1s^2 2s^2 2p^6 3d\ ^2D$. The $^2P_{1/2}$-$^2P_{3/2}$ fine-structure splitting was resolved for the final configuration $1s^2 2s^2 2p^6 3p$. The branching ratio for the transition to $1s^2 2s^2 2p^6 3d\ ^2D$, which involves three electrons and, thus, must be ascribed to correlation, is compared to earlier results for the isoelectronic ions Al^+ and Ar^{6+}. Good agreement between observed and calculated branching ratios to the three final states is obtained by including only correlation in the initial state. A discrepancy for the branching to the $1s^2 2s^2 2p^6 3d\ ^2D$ term, which was observed already in the earlier investigation of Ar^{6+}, has been removed by including correlation in the $n=2$ shell in addition to the correlation in the $n=3$ shell, which was the only correlation introduced previously.

PACS number(s): 32.80.Hd, 34.50.Fa

I. INTRODUCTION

High-resolution projectile Auger spectroscopy has become a powerful tool for obtaining detailed information about the structure of highly ionized atoms [1,2]. In particular, the method of zero-degree Auger spectroscopy has been used extensively to study fast projectiles whose charge state may be prepared prior to the collision [3–6]. This method greatly reduces Doppler broadening which has a deteriorating effect on the resolution in Auger spectroscopy at high-projectile energies and the method provides as a result excellent energy resolution. Furthermore, when using light target atoms, such as He, the projectile ion can be ionized selectively. The low-Z target acts like a "needle" which leaves the outer shell undisturbed in the process of ionizing the inner shell of the projectile. Hence, the ground-state structure may be retained in the outer shells of the projectile, and as a result the number of different Auger decays produced in the collision is reduced.

The method of "needle ionization" is particularly well suited for many-electron systems whose Auger spectra are so complex that a detailed analysis is difficult to perform. For instance, this method has successfully been applied to measure L-Auger spectra of open-shell ions with more than ten electrons. Already the first L-shell Auger studies [3] of the Ar^{5+} + He collision system using zero-degree spectroscopy showed that spectra of remarkable simplicity are produced. The spectra consisted of well-separated lines associated with the decay of states belonging to the configuration $1s^2 2s^2 2p^5 3s^2 3p$ in Mg-like Ar^{6+}, which was produced by selective ionization of the 2p shell. (Hereafter, the passive $1s^2$ shell will be left out of the configuration labels.) Two intensive peak groups were identified [3] as being due to transitions to the final states $2s^2 2p^6 3s$ and $2s^2 2p^6 3p$. A third peak group, less intensive but still significant, was later associated [7] with transitions to the final state $2s^2 2p^6 3d$. An analogous peak group has been observed in the decay of the $2s^2 2p^5 3s^2 3p$ configuration in Al^+ by Malutzki *et al.* [8] using photoionization to produce the initial state. This peak group is remarkable since it is due to three-electron transitions which involve second-order effects of the electron-electron interaction.

Recently, a detailed study of the L-Auger spectrum of

Ar^{6+} has been carried out by Focke *et al.* [6] The measured Auger lines were compared with theoretical results for Auger energies and decay rates evaluated by means of the configuration-interaction code due to Cowan [9] using Hartree-Fock basis states. The experimental line intensities associated with the final configuration $2s^22p^63s$ and $2s^22p^63p$ were found to be in reasonable agreement with the transition rate calculations (in conjunction with the assumption of a statistical population of the initial states). However, for the decay to the final configuration, $2s^22p^63d$, the agreement between experiment and theory was worse in Ar^{6+} than in Al^+. At first sight this discrepancy is perhaps not so surprising since the decay is due exclusively to correlation and thus inherently more difficult to calculate than the decays to $2s^22p^63s$ and $3p$. Only correlation within the $n=3$ part of the complex [10] to which the initial state belongs was considered in the calculations, i.e., the mixing of $2s^22p^53s^23p$ with configurations like $2s^22p^53s3p3d$ and $2s^22p^53p3d^2$, while the final states were considered to be pure. For the final ionic states this assumption is reasonable but it may well be that effects such as interchannel configuration interaction in the final state [2], e.g., bétween $2s^22p^63d\epsilon s$ and $2s^22p^63p\epsilon p$ are important also. However, if the discrepancy was due to interchannel configuration interaction the discrepancy would be expected to be larger in Al^+ than in Ar^{6+}, since interchannel configuration interaction is expected to be more important for small values of the free-electron energy. This expectation does not agree with the discrepancies between experiment and theory. For Al^+ the calculated intensity to $2p^63d$ (summed over the initial states) is 25% *smaller* than the experimental value [8]. On the contrary, the theoretical value for Ar^{6+} is *larger* (by nearly a factor of 2) than the experimental results [6]. In view of this apparent inconsistency we felt that further work was needed to study the three-electron transition in Mg-like ions.

In the present work we measured scandium L-Auger electrons produced in 89-MeV Sc^{8+} + He collisions using the method of zero-degree Auger spectroscopy. As for the isoelectronic system Ar^{5+} + He, a detailed theoretical analysis of the measured line energies and intensities is performed. The fine-structure splitting in the final state $2s^22p^63p\ ^2P_{1/2,3/2}$ can be observed in the experiment so that individual transitions to the different final states can be studied. Particular attention is devoted to the three-electron transition to the final state $2s^22p^63d$. For this transition good agreement between experimental and theoretical results is obtained by means of improved calculations based on configuration interaction in the initial state as before but now including the interaction with states having a $2s$ vacancy, thus including interactions within the $n=2$ part of the complex also. The calculations also remove to a large extent the remaining discrepancy between experiment and theory in the case of Ar^{6+} but makes practically no difference to the previous results [8] for Al^+. As a result of the calculations, the deviations between theory and experiment follow the expected pattern of better agreement for highly ionized systems where interactions within the complex dominate over other types of correlations.

II. EXPERIMENTAL RESULTS

The experiments were performed at the tandem accelerator facility at the Japan Atomic Energy Research Institute of Tokai. The beam line used in the measurements has been described before [11]. Also, the experimental setup in the multipurpose scattering chamber has been presented recently [12] so that only a brief outline is given here. A beam of 89-MeV Sc^{8+} extracted from the tandem accelerator was analyzed by a bending magnet and focused into the scattering chamber. After collimation of the beam to a diameter of about 2 mm, a current of about 100 nA was directed through the target gas cell and collected in a Faraday cup. The target gas pressure in the cell was a few m Torr and the target length was about 5 cm. During operation of the cell the pressure in the scattering chamber was about 10^{-2} m Torr. The resulting target thickness was sufficiently thin to guarantee single collision conditions.

The Auger electrons produced in the target gas cell were measured under an observation angle of 0° relative to the incident beam direction. The electron spectrometer is similar to that used by Itoh *et al.* [3]. The spectrometer consists of two parallel-plate electrostatic analyzers combined in tandem. The first analyzer is used as a deflector to separate the electrons from the ion beam. The second analyzer is used for the high-resolution measurements of the electrons. To improve the energy resolution, the electrons were decelerated in front of the second spectrometer. The deceleration voltage was varied in such a way that the electrons entering the second spectrometer had a constant energy. Therefore, the spectral structures were measured with a constant energy resolution in the laboratory frame of reference. In the measurement of the L-Auger spectrum of scandium the energy resolution was selected to be 3-eV full width at half maximum (FWHM). The Auger spectra, which were

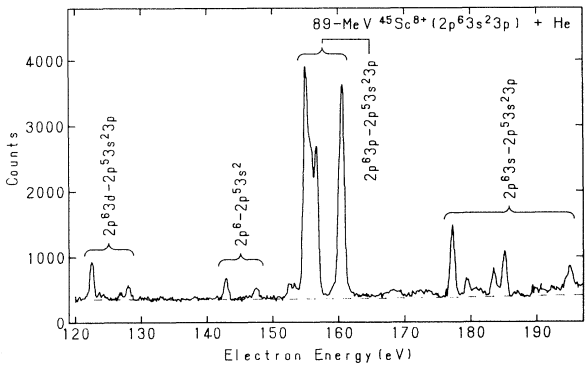

FIG. 1. L-shell Auger spectrum of Sc produced in collisions of 89-MeV Sc^{8+} ions on He. The observation angle is 0°. The electron energy refers to the projectile frame. Three groups of lines are assigned to the transitions from the initial configuration $2p^53s^23p$ of Sc^{9+} to the final ones $2p^63d$, $2p^63p$, and $2p^63s$, respectively. Two lines result from the decay of the doublet $^2P_{3/2}$-$^2P_{1/2}$ attributed to the configuration $2p^53s^2$.

measured in the laboratory frame near 1850 eV, were transformed into the projectile frame of reference where energies of about 150 eV were obtained. Relativistic effects [12] were accounted for in this Doppler transformation. Besides the Doppler shift, a kinematic compression [2] of the spectral linewidths occurs and, thus, the energy resolution is improved to 0.78 eV (FWHM) near 180 eV in the projectile frame of reference. This resolution was sufficient to resolve most of the spectral structures.

Figure 1 shows an example of the transformed L-Auger spectrum produced in 89-MeV $Sc^{8+}+He$ collisions. The spectral structures are well understood in terms of theoretical results described further below. The spectrum exhibits a pair of peaks at 143.5 and 147.8 eV which are attributed to the transitions from the $^2P_{3/2}$-$^2P_{1/2}$ doublet formed by the initial configuration $2s^22p^53s^2$ in the Sc^{10+} ion to the final state $2s^22p^6$. The production of this doublet shows that in some collisions the $3p$ electron has been removed in addition to the ionization of the $2p$ electron. The fraction of the total intensity of the spectrum due to the $^2P_{3/2}$-$^2P_{1/2}$ doublet is only 7%, showing that, if the Auger decay is isotropic, there is a relatively small deviation from the assumption of selective $2p$ ionization. This fraction should be compared to the value of 10% obtained [6] in collisions between 80-

TABLE I. Energies and intensities of L-Auger lines of Sc^{9+}. The initial states are specified by the largest LSJ component in the eigenvector. The theoretical values were calculated with the configuration-interaction Hartree-Fock program of Cowan (Ref. [9]). For the theoretical intensities a $2J+1$ population of the initial states was assumed. The theoretical and experimental intensities are normalized to the same total value of 100. The absolute and relative values of the experimental energies are uncertain by 0.5 and 0.2 eV, respectively. [It is recalled that the notation, e.g., 7.7(20) stands for 7.7±2.] The theoretical energies are normalized by setting the theoretical mean energy value equal to the corresponding experimental result.

Transition	Energy (eV)		Relative intensity (%)		
	Theory[a]	Expt.	Theory[b]	Theory[a]	Expt.
Final configuration: $2s^22p^63s$					
$^2S_{1/2}$-$^3S_1$	177.29	177.2	6.35	6.32	6.6(4)
$^2S_{1/2}$-$^3D_2$	179.44	179.5	1.27	0.61	1.9(2)
$^2S_{1/2}$-$^3D_3$	179.57		1.80	0.94	
$^2S_{1/2}$-$^1P_1$	180.53	180.5	0.89	0.78	0.65(20)
$^2S_{1/2}$-$^3P_2$	181.11	181.2	1.52	0.15	0.72(20)
$^2S_{1/2}$-$^3P_0$	183.44	183.5	2.64	2.54	2.3(5)
$^2S_{1/2}$-$^3D_1$	183.92	183.9	0.53	0.25	0.52(20)
$^2S_{1/2}$-$^3P_1$	184.97	185.0	4.17	3.73	4.2(4)
$^2S_{1/2}$-$^1D_2$	185.02		1.30	0.54	
$^2S_{1/2}$-$^1S_0$	194.92	194.8	2.66	2.63	2.1(6)
Final configuration: $2s^22p^63p$					
$^2P_{3/2}$-$^3S_1$	152.74	152.6	1.42	1.26	1.4(6)
$^2P_{1/2}$-$^3S_1$	153.57	153.4	0.57	0.75	1.3(3)
$^2P_{3/2}$-$^3D_2$	154.89	155.0	4.67	2.62	20.5(15)
$^2P_{3/2}$-$^3D_3$	155.02		14.21	16.04	
$^2P_{1/2}$-$^3D_2$	155.72	155.6	5.51	9.14	6.5(20)
$^2P_{1/2}$-$^3D_3$	155.85	155.9	0.17	0.21	7.7(20)
$^2P_{3/2}$-$^1P_1$	155.98		5.54	5.19	
$^2P_{3/2}$-$^3P_2$	156.56	156.7	5.13	12.9	11.0(15)
$^2P_{1/2}$-$^1P_1$	156.81	156.8	1.21	1.96	2.3(10)
$^2P_{1/2}$-$^3P_2$	157.39	157.5	0.84	0.23	0.13(8)
$^2P_{3/2}$-$^3P_0$	158.89	158.9	0.064	0.23	0.88(10)
$^2P_{3/2}$-$^3D_1$	159.37	159.4	0.40	0.52	0.23(8)
$^2P_{1/2}$-$^3P_0$	159.72	159.7	0.066	0.0003	1.4(5)
$^2P_{1/2}$-$^3D_1$	160.20	160.2	6.38	6.90	8.2(16)
$^2P_{3/2}$-$^3P_1$	160.42	160.5	1.66	3.68	12.6(15)
$^2P_{3/2}$-$^1D_2$	160.47		5.37	10.74	
$^2P_{1/2}$-$^3P_1$	161.25	161.3	2.43	0.88	0.91(20)
$^2P_{1/2}$-$^1D_2$	161.30		4.42	1.10	
$^2P_{3/2}$-$^1S_0$	170.37	170.3	0.080	0.094	0
$^2P_{1/2}$-$^1S_0$	171.20	171.1	0.040	0.053	0
Final configuration: $2s^22p^63d$					
$^2D_{5/2}$-$^3S_1$	120.25	120.2	0.003	0.003	0.02(2)
$^2D_{3/2}$-$^3S_1$	120.33		0.004	0.003	

TABLE I. (*Continued*).

Transition	Energy (eV) Theory[a]	Energy (eV) Expt.	Relative intensity (%) Theory[b]	Relative intensity (%) Theory[a]	Relative intensity (%) Expt.
$^2D_{5/2}$-$^3D_2$	122.40		0.40	0.31	
$^2D_{3/2}$-$^3D_2$	122.47	122.5	2.04	1.20	3.4(4)
$^2D_{5/2}$-$^3D_3$	122.53		3.26	2.24	
$^2D_{3/2}$-$^3D_3$	122.60		0.004	0.005	
$^2D_{5/2}$-$^1P_1$	123.49	123.5	0.013	0.011	0.41(10)
$^2D_{3/2}$-$^1P_1$	123.57		0.68	0.39	
$^2D_{5/2}$-$^3P_2$	124.07	124.2	5.42	0.51	0.41(10)
$^2D_{3/2}$-$^3P_2$	124.15		0.99	0.135	
$^2D_{5/2}$-$^3P_0$	126.40	126.4	0.004	0.003	0.05(5)
$^2D_{3/2}$-$^3P_0$	126.47		0.0001	0.0001	
$^2D_{5/2}$-$^3D_1$	126.88	126.9	0.002	0.002	0.52(15)
$^2D_{3/2}$-$^3D_1$	126.96		1.01	0.66	
$^2D_{5/2}$-$^3P_1$	127.93		0.021	0.012	
$^2D_{5/2}$-$^1D_2$	127.98	128.0	2.24	1.12	1.2(2)
$^2D_{3/2}$-$^3P_1$	128.00		0.050	0.025	
$^2D_{3/2}$-$^1D_2$	128.05		0.55	0.38	
$^2D_{5/2}$-$^1S_0$	137.88	137.8	0.002	0.002	0
$^2D_{3/2}$-$^1S_0$	137.96		0.001	0.001	
	Sum of all intensities:		100	100	100

[a] $n=2$ and 3 correlation included in the initial state.
[b] Only $n=3$ correlation included in the initial state.

MeV Ar^{5+} ions and He.

The remainder of the spectral intensity is due to the initial configuration $2s^22p^53s^23p$ of Mg-like Sc^{9+} which is produced by ionization of a single $2p$ electron in the ground-state configuration $2s^22p^63s^23p$ of Sc^{8+}. The three peak groups with centroid energies near 125, 157, and 181 eV are associated with transitions to the final-state configurations $2s^22p^63d$, $2s^22p^63p$, and $2s^22p^63s$, respectively. The structure in each feature is produced primarily by the level splitting in the initial state due to the interaction of the $2p$ hole with the $3p$ electron. In the intermediate coupling scheme, this interaction gives rise to ten states. The analysis of the individual decay schemes for each of these states is the major task of this work.

To obtain information about the excitation probability and the branching ratios for the initial states associated with the Mg-like configuration we decomposed the three line groups into their individual components. Before fitting we subtracted a smooth continuous background which results from other electron emission processes such as direct ionization. Since the natural width of the Auger lines was calculated to be less than 0.02 eV for all the lines in the spectrum, except for the line associated with the $^1S_0$ level as discussed later, we could fit all lines with one line shape which is identical to the spectrometer response function. The results of the line fit are given in Table I, which shows energies and the relative intensities of the measured lines. In some cases individual lines could not be resolved. Lines are clustered into groups when they lie within about 0.2 eV of each other.

III. THEORETICAL RESULTS

Theoretical data for transition energies and decay rates were obtained using the configuration-interaction Hartree-Fock (CIHF) program due to Cowan [9]. At first, calculations of the same type as performed for Ar^{6+} were carried out for Sc^{9+}. When it turned out that the calculated $3d$ intensity (17%) was even further from the experimental value (6%) than in Ar^{6+}, we realized that a new idea was necessary. In the calculations we had included the interactions in the initial state with configurations having three $n=3$ electrons while keeping the $2s^22p^5$ core fixed. In addition, since it is known [13] that the $2p^53p\ ^1S$ term cannot be described by the same set of radial integrals as the rest of the $2p^53p$ terms, we included other bound configurations of the type $2p^5np$ which are known to be able to remedy this defect. However, for a correct description it is necessary to include a complete set of $2p^5p'$ configurations including continuum ones [14] although the need for the latter should decrease with increasing ionization. This expectation is confirmed by the following observation. In order to get agreement between observed and calculated energies, in particular for the distance between the high-lying $^1S_0$ term and the rest of the terms in the configuration, it is necessary to reduce the exchange integrals by a factor which in the earlier studies [8,6] was determined by trial and error to be about 10%. This procedure is believed to correct for the fact that the basis set used includes only a finite num-

ber of configurations and in particular no continua [14]. The most important exchange integral, $G^0(2p,3p)$, has a pronounced effect on the energy of the $^1S_0$ term, while it does not influence the energies of the other terms in the p^5p' configuration to first order. In the case of Sc^{9+} we have found that a reduction of 5% gives the best agreement with the observed energies, as described later. Since the scaling factor seems to be approaching 1 with increasing ionization, it is unlikely that deficiencies in this treatment can be the reason for the deterioration in the agreement for the decay rates. We tried to improve on the description by adding excited configurations of the type $2p^53s^2np$ $(n>5)$ and $2p^53p^2np$ $(n>3)$, which were not considered in the previous calculations [8,6], but the resulting effect on the decay rates was negligible as expected.

It is important to keep in mind, however, that although the decay to $2p^63d$ is about 10% of the total decay rate, this is caused by very small admixtures (less than 2%) of perturbing configurations with one or two $3d$ electrons. Thus, it can be expected that very small admixtures of configurations omitted in the analysis can be equally important. We realized that, although the distance between configurations with a $2s$ hole compared to those with a $2p$ hole is rather large, the mixing due to configurations with a $2s$ hole in the wave-function expansion can have an effect on the decay rate to $2s^22p^63d$. In other words, while the previous calculations included only the mixing within the $n=3$ part of the complex to which $2s^22p^53s^23p$ belongs, the present calculations include all configurations within the whole complex plus the excited np configurations mentioned earlier. As expected, the configurations within the complex are the most important ones in the highly ionized system Sc^{9+}. The resulting wave-function expansion is as follows:

$$2s^22p^53s^2(3p+4p+5p+6p)$$
$$+2s^22p^5(3s3p3d+3p3d^2+3p^3+3p^24p+3p4p^2)$$
$$+2s2p^6(3s^23d+3d^3+3p^23d+3s3p^2)\,.$$

With this expansion a scaling factor of 95% for the exchange integrals was found to give the best agreement with the experimental energies for the $2s^22p^53s^23p$ configuration in Sc^{9+}, as was mentioned already.

As in the previous calculations, for Ar^{6+} we used the approximate relativistic Hartree-Fock (HFR) method, due to Cowan and Griffin [15], to construct the basis states since we expect that relativistic effects cannot be neglected for multiply ionized scandium. Since the spin-orbit parameter for the $2p$ electron is one of the most important interaction parameters, the calculations were performed within the intermediate coupling scheme. To distinguish the resulting states we used the largest LS term component as a label. In Ar^{6+} the labeling in the LS scheme was ambiguous [6], but in Sc^{9+} this problem did not occur. However, the purity of the eigenvector compositions is not very high. It is also observed that the ordering of the energy levels for some of the close-lying levels differ between argon and scandium as can be expected when the eigenstates are very mixed. The results of the energy calculations are shown in Table I and Fig. 2, in comparison with the experimental data. For an absolute calibration of the calculated data, the theoretical mean value of the line energies weighted by their intensity were set to be equal to the corresponding experimental value. The relative theoretical energies between the final configurations $2s^22p^63s$, $2s^22p^63p$, and $2s^22p^63d$ are obtained by subtracting the tabulated excitation energies [16] for the $3p$ and $3d$ electrons from the $2s^22p^53s^23pSLJ$-$2s^22p^63s$ energies. The relative splittings within the $2s^22p^53s^23p$ configuration is well described by the calculations which, as mentioned, include only *one* semiempirical scaling factor, namely the 5% reduction of the exchange integrals.

The transition rate calculations were performed by means of perturbation theory using the CIHF code written by Cowan [9]. From the transition rates we determined branching ratios for a given initial state to the final states $2s^22p^63s\ ^2S_{1/2}$, $2s^22p^63p\ ^2P_{1/2}$, $2s^22p^63p\ ^2P_{3/2}$, $2s^22p^63d\ ^2D_{3/2}$, and $2s^22p^63d\ ^2D_{5/2}$. The branching ratios were multiplied by $2J+1$, where J is the total angular momentum of the initial state, which is equivalent to assuming a statistical population of the initial levels. Finally, the sum of the individual rates was normalized to the overall intensity of 100. The same normalization pro-

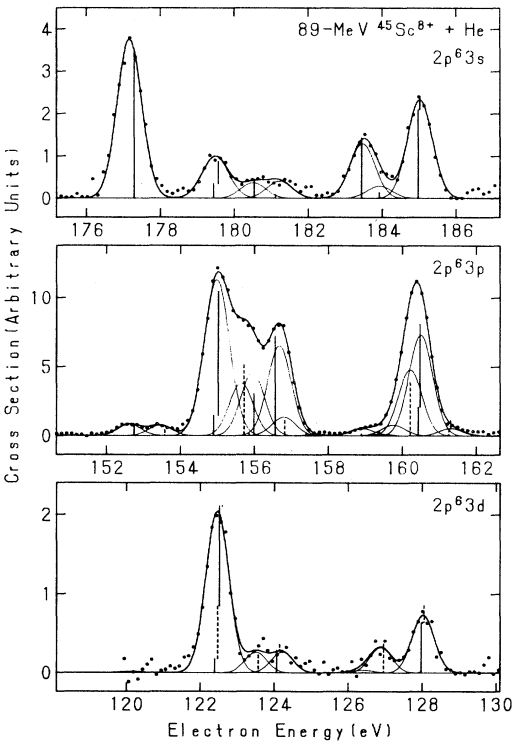

FIG. 2. Line structure of Auger transition spectra from Sc^{9+}. The initial configuration is $2p^53s^23p$ and the final configurations are $2p^63s$, $2p^63p$, and $2p^63d$ as indicated on the spectra. The position and length of the vertical solid and dashed lines represent theoretical transition energies and intensities, respectively, as given in Table I. The solid lines represent fit curves resulting from the deconvolution of the experimental data; see text.

cedure was used for the experimental data shown in Table I. This was done to allow a direct comparison of experimental and theoretical line intensities. In the table we include both the results of the calculation carried out in the same way as for Ar^{6+} and of the present calculation, which includes the $2s$-$2p$ correlation. Although this correlation is minor, it is seen to have an appreciable effect on the decay rates, in particular, for the decay to $2s^2 2p^6 3d$. Since the initial populations are unknown, only the branching ratios for resolved levels can be compared unambiguously with experiment.

IV. DISCUSSION OF THE RESULTS

Table I and Fig. 2 indicate excellent agreement between the theoretical and experimental transition energies within the (relative) experimental uncertainty of 0.2 eV. (It should be recalled that the theoretical data are calibrated to fit the average experimental transition energies.) The good agreement for the transition energy of the isolated line attributed to the decay of the initial $^1S_0$ state to $2s^2 2p^6 3s\ ^2S_{1/2}$ is, however, due to the choice of scaling factor for the exchange integrals. This initial $^1S_0$ state is pushed to higher energies due to the large effect of exchange interaction for this term [13].

The main subject of the present work is the study of the line intensities associated with states of the initial configuration $2s^2 2p^5 3s^2 3p$. Due to the fact that the fine-structure splitting is significant in the case of the final state $2s^2 2p^6 3p\ ^2P_{1/2,3/2}$, it was important to determine the decay rates to the individual J levels of the final terms in order to be able to interpret the experimental results. It can be seen from Table I that the splitting of the final $3p$ state is important for the grouping of individual lines into unresolved features in the experimental spectrum. If this splitting is neglected, the interpretation of the experimental spectrum is much less successful. From Table I it is seen that fair agreement is obtained between the theoretical and experimental line intensities where we have compared intensities summed over closely lying levels. In the first set of calculations, including only the correlation within the $n=3$ shell, the decay to $2s^2 2p^6 3s$ is reasonably well described but, in particular, the decays of $2s^2 2p^5 3s^2 3p\ ^3P_2$ to $2s^2 2p^6 3p$ and $2s^2 2p^6 3d$ are seriously underestimated and overestimated, respectively. The same discrepancy was observed [6] for Ar^{6+}. This discrepancy has been removed in the final calculation and there is quite good agreement for the decay of this level, although the weak decay to $2s^2 2p^6 3s$ is underestimated. There are also some deviations in the final calculation, particularly for the decay to $2s^2 2p^6 3p$ most significant in relative terms for the weak decay from $^3P_0$. However, it should be kept in mind that part of the discrepancies may be due to the assumption of a statistical population of the initial levels. Nevertheless, we note that the agreement for the (weak) decays to $2s^2 2p^6 3s$ and, in particular, $3d$ is very good in the final calculation and systematically improved compared to the original calculation. The same is true for the (strong) decays to $3p$.

A direct verification of the statistical model is possible through the comparison of experiment and theory in the case of the initial $^1S_0$ level mentioned above. This state decays exclusively into the final $2p^6 3s\ ^2S_{1/2}$ state [8,6] so that branching ratios do not enter in the calculation of the line intensity. It is seen that the theoretical and experimental results agree well for this decay so that it can be concluded that the statistical excitation model is valid in this case. The analysis of the decay of the $^1S_0$ state was erroneous in the previous study [6] of the Mg-like Ar^{6+} ion. A revision of the Ar^{6+} data shows that the experimental line intensity for the Ar^{6+} ion agrees as well with the theoretical value as found in the case of Sc^{9+}. It is interesting to note that due to the strength of the (exchange) interaction determining the decay of the $^1S_0$ state [8], the transition rate for this state, 5.2×10^{14} sec^{-1}, is relatively large. It corresponds to a natural linewidth of 0.34 eV. This width is consistent with the difference between the measured linewidth of 0.95 eV and the width of the spectrometer function of 0.78 eV when assuming a quadratic rule for the summation of the associated linewidths.

In order to check the validity of the proposed explanation, we have repeated the calculations for Al^+ and Ar^{6+} using exactly the same expansion and also HFR basis states in both cases. We have also scaled the exchange integrals in this calculation down by 5% while 10% were used in the previous calculation [6]. The calculated transition probabilities for Al^+ differ only marginally from the previous results, but the present results for Ar^{6+} are in considerably better agreement with experiment than before. We show therefore (Table II) the present results for Ar^{6+} compared with the observations taken from the previous work [6], but including the present interpretation of the experimental results for $^1S_0$ mentioned earlier. As in Ref. [6], the absolute theoretical energies are normal- ized to the experimental energy of the $2s^2 2p^5 3s^2 3p\ ^3S_1 - 2s^2 2p^6 3s\ ^2S_{1/2}$ transition. The calculated energy differences agree with the previous ones to within 0.2 eV (i.e., within the experimental uncertainty) except for the $^1S_0$ level for which the absolute value of the deviation, 0.3 eV, is the same as before, although the sign is different (this is caused by the difference in scaling for the exchange integrals). The labels for two $J=1$ levels were ambiguous in the previous calculation [6]. The same is found here but the sensitivity of the mixing to the details of the calculation can be seen from the fact that we have interchanged the labels for these two levels as a result of the present calculation. The fine-structure splitting in the final states $2s^2 2p^6 3p\ ^2P$ and $2s^2 2p^6 3d\ ^2D$ are not resolved in the experiment [6], and we show in this case energies averaged over the splitting of the final states. The detailed comparison between observed and calculated intensities is closely similar to that for Sc^{9+}. For nearly all transitions, the present calculation is in better agreement with the observations than the original one. The main exceptions are found in the decay to $2s^2 2p^6 3p$. Part of these deviations might be due to the neglect of the splitting of the $3p\ ^2P$ term in the data analysis.

We compare in Table III calculated and observed branching ratios between the three final states for Al^+,

Ar^{6+}, and Sc^{9+}. The theoretical values are from the previous and the final calculation including full correlation in the complex. It can be seen that the data for Sc^{9+} agree within the uncertainties of the experiment while the agreement for Ar^{6+} is considerably improved, in particular for the branching to $2s^22p^63d$, while some deviations still exist for the decay to $3s$ and $3p$. For Al^+ the agreement is basically unchanged compared to the previous calculation [8], which could be expected since the $2s$-$2p$ energy difference is very large compared to other energies involved, for example the relatively small free-electron energies in this case. This means that it is reasonable to expect also other types of correlation to be important for Al^+. We note the tendency of the decay to $2s^22p^63p$ to become the dominant one with increasing ionization. The interaction integrals connecting the $2p^53s^23p$

TABLE II. Energies and intensities of L-Auger lines of Ar^{6+}. The experimental values are taken from Ref. [6] except that the decay of the $2s^22p^53s^23p\ ^1S_0$ level has been reanalyzed as explained in the text. The theoretical values were calculated with the configuration interaction Hartree-Fock program of Cowan (Ref. [9]). The calculations (b) include both $n=2$ and 3 correlation while the previous ones (Ref. [6]) (a), which are shown also, include only $n=3$ correlation. For the theoretical intensities, a $2J+1$ population of the initial states is assumed and the theoretical and experimental intensities are normalized to the same total value of 100. The absolute and relative values of the experimental energies are uncertain by 0.5 and 0.2 eV, respectively. The theoretical energies have been normalized to the experimental energy of the $2s^22p^53s^23p\ ^3S_1-2s^22p^63s\ ^2S_{1/2}$ transition.

Transition	Energy (eV)		Relative intensity (%)		
	Theory[a]	Expt.	Theory[b]	Theory[a]	Expt.
Final configuration: $2s^22p^63s$					
$^2S_{1/2}$-$^3S_1$	(126.70)[c]	126.7	6.37	6.42	5.5(4)
$^2S_{1/2}$-$^3D_3$	128.34	128.4	1.61	0.98	2.1(3)
$^2S_{1/2}$-$^3D_2$	128.46		1.30	0.88	
$^2S_{1/2}$-$^1P_1$	129.08	128.9	0.58	0.46	0.67(22)
$^2S_{1/2}$-$^3P_2$	129.45	129.5	3.64	2.93	1.7(2)
$^2S_{1/2}$-$^3D_1$	130.64	130.6	0.42	0.27	2.7(6)
$^2S_{1/2}$-$^3P_0$	130.65		2.59	2.58	
$^2S_{1/2}$-$^1D_2$	131.17	131.2	1.74[d]	1.37	3.8(5)
$^2S_{1/2}$-$^3P_1$	131.23		3.06	2.97	
$^2S_{1/2}$-$^1S_0$	138.90	138.6	2.66	2.63	2.2(5)[e]
Final configuration: $2s^22p^63p$					
^2P-$^3S_1$	109.11	109.2	1.97	1.91	1.9(3)
^2P-$^3D_3$	110.75	110.9	13.90	15.57	23.7(12)
^2P-$^3D_2$	110.87		9.76	10.98	
^2P-$^1P_1$	111.49	111.4	6.66	7.15	9.7(10)[d]
^2P-$^3P_2$	111.86	112.0	5.99	9.18	13.5(10)
^2P-$^3D_1$	113.05	113.1	6.90	7.28	4.2(8)
^2P-$^3P_0$	113.06		0.17	0.19	
^2P-$^1D_2$	113.58	113.7	9.01	10.46	20.6(1.3)
^2P-$^3P_1$	113.64		5.20	5.32	
^2P-$^1S_0$	121.31		0.12	0.14	0
Final configuration: $2s^22p^63d$					
^2D-$^3S_1$	85.45		0.007	0.005	0
^2D-$^3D_3$	87.09	87.3	3.84	2.90	4.7(6)
^2D-$^3D_2$	87.21		2.83	2.03	
^2D-$^1P_1$	87.83	87.8	1.08	0.73	0.29(9)
^2D-$^3P_2$	88.20	88.4	4.27	1.78	1.6(3)
^2D-$^3D_1$	89.39	89.5	1.05	0.79	0.78(18)
^2D-$^3P_0$	89.40		0.01	0.01	
^2D-$^1D_2$	89.92	90.1	3.17	2.06	2.0(2)
^2D-$^3P_1$	89.98		0.07	0.04	
^2D-$^1S_0$	97.65		0.004	0.003	0
Sum of all intensities:			100	100	100

[a] $n=2$ and 3 correlation included in the initial state.
[b] Only $n=3$ correlation included in the initial state (from Ref. [6]).
[c] Normalized to the experimental energy.
[d] Misprinted in the corresponding columns of Table II in Ref. [6].
[e] After a revised analysis of the experimental data from Ref. [6].

TABLE III. Intensities of Auger line groups attributed to different final states. The data are obtained by summing the intensities for the associated lines in Tables I and II. The theoretical and experimental intensities are normalized to the same total value of 100.

Final state	Theory[a]	Theory[b]	Expt.[c]
Al^+ ion			
$2s^22p^63s$	45	49	45
$2s^22p^63p$	43	40	39
$2s^22p^63d$	12	11	16
Ar^{6+} ion			
$2s^22p^63s$	24	21.5	18.4(10)
$2s^22p^63p$	60	68.2	72.4(20)
$2s^22p^63d$	16	10.3	9.2(10)
Sc^{9+} ion			
$2s^22p^63s$	23.1	18.5	19.0(10)
$2s^22p^63p$	60.1	74.5	75.0(20)
$2s^22p^63d$	16.8	7.0	6.0(8)

[a] Only $n=3$ correlation included in the initial state. Data for Al^+ and Ar^{6+} are from Refs. [8] and [6], respectively.
[b] $n=2$ and 3 correlation included in the initial state.
[c] Al^+ data are from Ref. [8]. Ar^{6+} data are taken from Ref. [6] after a revised analysis.

configuration to the $2s^22p^63s\epsilon s$ and $2s^22p^63p\epsilon p$ continua increase with increasing ionization while the integrals to the $2s^22p^63s\epsilon d$ continuum decrease. Only the S terms in $2s^22p^53s^23p$ can decay to the $2s^22p^63s\epsilon s$ continuum. These terms represent a small fraction of the initial population, when the population distribution is statistical, which explains the increase in the branching to $2s^22p^63p$.

V. CONCLUSIONS

We have measured Auger electron spectra of multiply charged scandium ions with high resolution. All the observed transitions could be identified with the help of CIHF calculations including relativistic corrections and interactions with the configurations in the complex to which the initial configuration $2s^22p^53s^23p$ belongs. In contrast to the earlier calculations, configurations with $2s$ holes belonging to the complex were also included and this turned out to explain discrepancies with the experimental branching ratios to the three final $2s^22p^63l$ configurations that had already been identified in a previous study [6] of the equivalent decay in Ar^{6+}. At the same time, we have found that the assumption of a statistical population of the levels of the initial configuration as a consequence of the collision is well fulfilled for both Ar^{5+} and Sc^{8+} + He collisions at energies in the region of 100 MeV. Thus we believe that as a result of our investigations these types of decays are rather well understood in terms of first-principles theories.

ACKNOWLEDGMENTS

One of us (N.S.) is much indebted to the Japan Atomic Energy Research Institute and the University of Tokyo for the support during his stay in Japan. The work of N.S. was performed also at the Laboratoire de Spectroscopie Atomique, ISMRA, Université de Caen, 14050 Caen, France. The CIHF calculations were performed on the CYBER 205 computer in Amsterdam under Grant No. SC-20 from the SURF foundation (the cooperative body for the advancement of computer services in higher education and scientific research).

*Present address: Department of Chemistry, Kyoto Institute of Technology, Matsugasaki, Kyoto 606, Japan.
†Present address: Institute of Nuclear Research, Bem tér 18c, H-4001 Debrecen P.F. 51, Hungary.

[1] I. A. Sellin, in *Beam Foil Spectroscopy,* edited by S. Bashkin, Topics in Current Physics Vol. I (Springer, Heidelberg, 1976), p. 265.
[2] N. Stolterfoht, Phys. Rep. **146**, 315 (1987).
[3] A. Itoh, T. Schneider, G. Schiwietz, Z. Roller, H. Platten, G. Nolte, D. Schneider, and N. Stolterfoht, J. Phys. B **16**, 3965 (1983); A. Itoh, D. Schneider, T. Schneider, J. T. M. Zouros, G. Nolte, G. Schiwietz, W. Zeitz, and N. Stolterfoht, Phys. Rev. A **31**, 684 (1985).
[4] D. Schneider, N. Stolterfoht, A. Itoh, G. Schiwietz, W. Zeitz, and U. Wille, in *Electronic and Atomic Collisions, Invited Papers,* edited by D. C. Lorents, W. E. Meyerhof, and J. R. Peterson (North-Holland, Amsterdam, 1986), p. 671.
[5] N. Stolterfoht, P. D. Miller, H. F. Krause, Y. Yamazaki, J. K. Swenson, R. Bruch, P. F. Dittner, P. L. Pepmiller, and S. Datz, Nucl. Instrum. Methods B **24/25**, 168 (1987).
[6] P. Focke, T. Schneider, D. Schneider, G. Schiwietz, I. Kádár, N. Stolterfoht, and J. E. Hansen, Phys. Rev. A **40**, 5633 (1989).
[7] N. Stolterfoht, T. Schneider, D. Schneider, and A. Itoh, in *XIVth International Conference on the Physics of Electronic and Atomic Collisions, Abstracts,* edited by M. J. Coggiola, D. L. Huestis, and R. P. Saxon (Stanford University Press, Stanford, 1985), p. 467.
[8] R. Malutzki, A. Wachter, V. Schmidt, and J. E. Hansen, J. Phys. B **20**, 5411 (1987).
[9] R. D. Cowan, *The Theory of Atomic Structure and Spectra* (University of California Press, Berkeley, 1981), Chaps. 7–14.
[10] D. Layzer, Ann. Phys. (N. Y.) **8**, 271 (1959).
[11] K. Kawatsura, M. Sataka, A. Ootuka, K. Komaki, H. Naramoto, K. Ozawa, Y. Nakai, and F. Fujimoto, Nucl. Instrum. Methods A **262**, 150 (1987).
[12] K. Kawatsura, M. Sataka, Y. Yamazaki, K. Komaki, Y. Kanai, H. Naramoto, K. Kuroki, T. Kambara, Y. Awaya, Y. Nakai, and N. Stolterfoht, Nucl. Instrum. Methods B **48**, 103 (1990).

[13] J. E. Hansen, J. Phys. B **6**, 1387 (1973).
[14] J. E. Hansen, Phys. Scr. **21**, 510 (1980).
[15] R. D. Cowan and D. C. Griffin, J. Opt. Soc. Am. **66**, 1010 (1976).
[16] J. Sugar and C. Corliss, J. Phys. Chem. Ref. Data **14**, Suppl. 2, 130 (1985); V. Kaufman and J. Sugar, J. Phys. Chem. Ref. Data **17**, 1679 (1988).